ELSEVIER

Journal of Fluids and Structures 25 (2009) 676–686

JOURNAL OF FLUIDS AND STRUCTURES

www.elsevier.com/locate/jfs

Floquet stability analysis of the flow around an oscillating cylinder

R.S. Gioria[a,*], P.J.S. Jabardo[a], B.S. Carmo[b], J.R. Meneghini[a]

[a]*NDF, POLI, University of São Paulo, Brazil*
[b]*Department of Aeronautics, Imperial College, London, UK*

Received 31 March 2008; accepted 16 January 2009
Available online 12 March 2009

Abstract

This investigative work is concerned with the flow around a circular cylinder submitted to forced transverse oscillations. The goal is to investigate how the transition to turbulence is initiated in the wake for cases with different Reynolds numbers (Re) and displacement amplitudes (A). For each Re the motion frequency is kept constant, close to the Strouhal number of the flow around a fixed cylinder at the same Re. Stability analysis of two-dimensional periodic flows around a forced-oscillating cylinder is carried out with respect to three-dimensional infinitesimal perturbations. The procedure consists of performing a Floquet type analysis of time-periodic base flows, computed using the spectral/*hp* element method. With the results of the Floquet calculations, considerations regarding the stability of the system are drawn, and the form of the instability at its onset is obtained. The critical Reynolds number is observed to change with the amplitude of oscillation. With respect to instabilities, unstable modes with the same symmetry as mode A of a fixed cylinder are observed; however, they present different wavelengths. Also, the instabilities observed for the oscillating cylinder are distinctively stronger in the braid shear layers. Other unstable modes similar to mode B are found. Quasi-periodic modes are observed in the 2S wake, and subharmonic mode occurrences are reported in P + S wakes.

Keywords: Secondary wake transition; Floquet analysis; Oscillating cylinder

1. Introduction

The phenomena involved in vortex-induced vibration are still the subject of many studies due its significant involvement in practical engineering. The phenomena still have some unanswered questions with physical relevance. The oscillation of the circular cylinder does affect the wake transition and the three-dimensional unstable mode of the wake and may be a key characteristic of free oscillations of high amplitude.

The flow around a forced-oscillating circular cylinder has been studied extensively with focus on the shedding regime, phase angle between body displacement and transverse force, for example Bearman and Currie (1979), Griffin et al. (1973), Griffin and Ramberg (1974), and Blackburn and Henderson (1999). Detailed observations of three-dimensional instabilities of the wake of a circular cylinder have been in focus and reported since Williamson (1988), who observed a two-stage transition of the wake by noticing the discontinuities of the Strouhal versus Reynolds number curve.

*Corresponding author. Tel.: +55 11 3091 5724; fax: +55 11 3813 1886.
E-mail address: rafael.gioria@poli.usp.br (R.S. Gioria).

0889-9746/$ - see front matter © 2009 Elsevier Ltd. All rights reserved.
doi:10.1016/j.jfluidstructs.2009.01.004

The modes A and B noticed in his work were also reproduced in several other numerical simulations; see for instance Wu et al. (1994), Zhang et al. (1995), and Thompson et al. (1996). Mode A is a spanwise periodic three-dimensional flow structure with a wavelength of $\approx 4d$ (d is the diameter of cross-section) and mode B is also a spanwise periodic wake structure of wavelength $\approx 0.8d$. These three-dimensional instabilities were obtained through Floquet stability analysis by Barkley and Henderson (1996) (Iooss and Joseph, 1990) in good agreement with the spanwise wavelength and the critical Reynolds number observed in the experiments: $\mathrm{Re}_{\mathrm{cr}} \approx 188$ for mode A and $\mathrm{Re}_{\mathrm{cr}} \approx 260$ for mode B.

There are several other three-dimensionalities reported in wakes of bluff bodies: one not found in the wake of a fixed circular cylinder, although reported for staggered circular cylinders' arrangements and a single oscillatory circular cylinder, is called mode C. Mode C has a typical intermediary spanwise periodic length, but interestingly it exhibits subharmonic properties where the three-dimensional features alternates sign at each shedding cycle (period-doubling characteristic). Floquet stability analysis of ring wakes (Sheard et al., 2003) and of two circular cylinders in staggered arrangements (Carmo et al., 2008) produced mode C in certain situations.

The mode C seems to occur when the two-dimensional wake does not present a spatio-temporal symmetry of the $\mathscr{H}(u,v)(x,y,t) = \mathscr{H}(u,-v)(x,y,t+\frac{1}{2}T)$ kind (half period time shift and spatial reflection about wake centerline). This kind of symmetry is found in a typical von Kármán vortex street, for example. Hence, for the occurrence of mode C in a single circular cylinder wake, a symmetry breaking mechanism is needed. This mode was observed on wakes of a single circular cylinder in experiments and computations in which this symmetry was broken, for example, with a trip wire as in Zhang et al. (1995). Another way to observe the symmetry breaking is to impose a transverse oscillation to the circular cylinder. This has been observed by means of DNS (Gioria et al., 2007b; Gioria and Meneghini, 2007) and Floquet stability analysis (Leontini et al., 2007; Gioria et al., 2007a).

Another possible mode in oscillating circular cylinder wakes is a quasi-periodic mode: when the instability contains an imaginary component. The quasi-periodic instability leads to travelling or standing waves for the three-dimensional modes.

The mechanism of instability deflagration and sustainability is not well understood. Steps towards the understanding of the physical mechanism of the instabilities (Williamson, 1996; Leweke and Williamson, 1998) have reached a proposal that mode A originates in the near wake vortex cores and mode B in the near wake braided shear layers. A physical mechanism for mode C has already been proposed as a hybrid of the mechanisms of modes A and B by Sheard et al. (2005). Non-linear characteristics of the transition of the wake of a fixed circular cylinder have been assessed (Henderson and Barkley, 1996; Henderson, 1997): mode A seems to bifurcate through a subcritical route and mode B through a supercritical one.

This paper means to characterize the wake transition of an oscillating circular cylinder, keeping the ratio frequency f/f_s constant, where f is the imposed oscillation frequency and f_S is the Strouhal frequency of a fixed circular cylinder. The rise of the instability is identified by means of Floquet stability analysis of the two-dimensional time-periodic base flows. The results are compared to those of a fixed circular cylinder.

2. Methodology

2.1. Direct numerical simulation

We consider the flow of a viscous fluid past around a circular cylinder placed perpendicular to an uniform free stream. The fluid is assumed to have constant dynamic viscosity μ. The incompressible flow depends on three-dimensional parameters: the cylinder diameter d, the free-stream speed U, and the kinematics viscosity of the fluid ν. So we take the Reynolds number, $\mathrm{Re} = Ud/\nu$, to act as the control parameter for the system. The problem may be described in dimensionless variables with U and d serving as the reference scales for velocity and length. The state of the fluid at any instant t, as it moves past the cylinder, is determined by the velocity field $\mathbf{u}(x,y,z,t)$ ($\mathbf{u}(x,y,t)$ for two-dimensional simulations) and the pressure field $p(x,y,z,t)$ ($p(x,y,t)$ for two-dimensional simulations). The resulting non-dimensional equations that govern the proposed problem are

$$\frac{\partial \mathbf{u}}{\partial t} = -(\mathbf{u}\cdot\nabla)\mathbf{u} - \nabla p + \frac{1}{\mathrm{Re}}\nabla^2\mathbf{u}, \tag{1}$$

$$\nabla\cdot\mathbf{u} = 0. \tag{2}$$

The spectral/hp method presented in Karniadakis and Sherwin (1999) is employed to numerically solve the incompressible Navier–Stokes equations. Ninth-degree polynomials are employed as basis functions in the two-dimensional simulations. In the three-dimensional simulations, the same polynomials are used in the cross-sectional

planes while Fourier expansion is used in the spanwise direction. A second order stiffly stable time-stepping scheme as described in Karniadakis et al. (1991) is employed to advance the solution in time.

To simulate the oscillatory movement of the body, an oscillatory cross-flow around circular cylinder in a frame of reference fixed to the body has been employed. The frame of reference fixed to the oscillating body is used for the simulations taking advantage of a non-deformable mesh in spectral/*hp* method. The uniform flow is superimposed on a cross-flow representing the transverse movement of the body, modifying the Dirichlet boundary conditions (upstream and side boundaries) and adding the oscillatory component ($\boldsymbol{\alpha}$) like in Li et al. (2002). In addition, an inertial acceleration field needs to be added to the vertical momentum equation. The modified equation with respect to the non-inertial frame of reference is (a distinct notation for the non-inertial frame of reference is not used for the sake of clarity)

$$\frac{\partial \mathbf{u}}{\partial t} = -(\mathbf{u}\cdot\nabla)\mathbf{u} - \nabla p + \frac{1}{\mathrm{Re}}\nabla^2\mathbf{u} + \boldsymbol{\alpha}, \tag{3}$$

$$\nabla\cdot\mathbf{u} = 0. \tag{4}$$

It is worth noting that the vorticity is not modified since the moving frame does not rotate and the outflow condition in the downstream boundary does not need changes.

2.2. Floquet stability analysis

Floquet stability analysis is similar to linear stability analysis of steady base flows. The main difference is how to deal with the periodic base flow. In the Floquet analysis, the growth of the small perturbations are evaluated with respect to the period of the base flow. So we evaluate an eigenproblem on the operator that evolves the perturbation to the next period of the flow. Each eigenvalue of this operator shows the growth/decay rate of the perturbation over a period: these are the Floquet multipliers (μ). When $|\mu|>1$, the flow is unstable and the perturbation grows each period. The associated eigenvector is the Floquet mode which represents the growing perturbation field. Otherwise if $|\mu|<1$, the flow is stable to three-dimensional perturbations.

More information, beyond growth/decay rate, is present in the Floquet multiplier. The perturbation field, as a period goes by, is multiplied by the Floquet multiplier (see definition in the next section). So if the Floquet multiplier is real and positive, the perturbation field is only altered by a growth/decay rate. If the Floquet multiplier is real and negative, the perturbation field also suffers a change in its sign. In order to have its initial sign back, another period needs to go by, thus the period of the perturbation field is twice the period of the base flow. This is referred as a subharmonic mode in this paper, with a period-doubling characteristic. If the Floquet multiplier is complex, it means it introduces a non-harmonic frequency over the base flow. Usually, for the wake of a circular cylinder, these modes can be observed as a standing or travelling waves in the spanwise direction.

After we employ the Floquet theory to the linearized equations for the perturbation evolution, we assume that the spanwise direction is homogeneous (an infinite long cylinder) and we use a Fourier expansion in the spanwise direction to represent the perturbation field since we are interested in the three-dimensional perturbations of the flow. In the linearized equations for the perturbation evolution, each Fourier component of the expansion is independent of the others, therefore we evaluated each wavelength λ (or wavenumber $\beta = 2\pi/\lambda$) of the Fourier expansion independently.

In each case presented in this investigation, we look for Floquet multipliers which are greater than 1 in a range of wavenumbers. Actually, we are interested in the wavenumbers which have the largest growth rate, hence we seek the peaks on the plots of Floquet multiplier (μ) × wavenumber (β). These peaks are the most unstable modes that govern the dynamics in the asymptotic behavior of the linearized system.

2.2.1. Floquet method description

We consider a periodic two-dimensional base flow $\mathbf{U}(x,y,t)$, with period T, and verify its stability to a three-dimensional perturbation $\mathbf{u}'(x,y,z,t)$. The equations that govern the perturbation evolution, at first order, are the linearized Navier–Stokes equations:

$$\frac{\partial \mathbf{u}'}{\partial t} = -(\mathbf{U}\cdot\nabla)\mathbf{u}' - (\mathbf{u}'\cdot\nabla)\mathbf{U} - \nabla p' + \frac{1}{\mathrm{Re}}\nabla^2\mathbf{u}', \tag{5}$$

$$\nabla\cdot\mathbf{u}' = 0, \tag{6}$$

where p' is the perturbation to the pressure. The boundary conditions for those equations are $u' = 0$ on the walls and inlet, and the outflow condition (the same as for the base flow calculations) on the boundary downstream of the cylinder.

The right-hand side of Eq. (5) subject to the incompressibility constant of Eq. (6) can be represented by an operator $\mathbf{L}$, so we can write the evolution equation in a compact form

$$\frac{\partial \mathbf{u}'}{\partial t} = \mathbf{L}(\mathbf{u}'). \tag{7}$$

The operator $\mathbf{L}(\mathbf{u}')$ is T-periodic because it depends on the base flow $\mathbf{U}(x, y, t)$, which is T-periodic. Therefore, the stability of (7) can be determined using Floquet analysis. The solutions of (7) can be decomposed into a sum of solutions of the form $\tilde{\mathbf{u}}(x, y, z, t)e^{\sigma T}$, where $\tilde{\mathbf{u}}(x, y, z, t)$, which are called Floquet modes, are T-periodic solutions. The complex exponents σ are the Floquet exponents, and the sign of their real parts determines the stability of the system. However, in Floquet type problems it is more usual to consider the Floquet multiplier $\mu \equiv e^{\sigma T}$ instead of the Floquet exponent. If the Floquet multiplier is located inside the unit circle ($|\mu|<1$), then the three-dimensional perturbation will decay exponentially with time, and if the multiplier is located outside the unit circle ($|\mu|>1$), this means that the three-dimensional perturbation will grow exponentially with time, and the system is unstable.

Due to the fact that the system is homogeneous in the spanwise direction z, a further simplification can be made. A perturbation of the velocity field can be expressed in terms of the Fourier integral:

$$\mathbf{u}'(x, y, z, t) = \int_{-\infty}^{\infty} \hat{\mathbf{u}}(x, y, \beta, t)e^{i\beta z}\, d\beta, \tag{8}$$

and similarly for p', where the wavenumber $\beta = 2\pi/\lambda$ (λ is the wavelength of the instability). Since Eq. (7) is linear, modes with different β do not couple, and perturbations of the form

$$\mathbf{u}'(x, y, z, t) = (\hat{u}\cos\beta z, \hat{v}\cos\beta z, \hat{w}\sin\beta z), \tag{9}$$

$$p'(x, y, z, t) = \hat{p}\cos\beta z, \tag{10}$$

remain of this form under this operator. Thus, the Floquet modes $\tilde{\mathbf{u}}(x, y, z, t)$ will necessarily be of this same form. As the velocity components $(\hat{u}, \hat{v}, \hat{w})$ and pressure $\hat{p}$ depend only on x, y and t, the three-dimensional stability problem can be reduced to a series of two-dimensional stability problems, by varying the value of β. Consequently, the stability of the two-dimensional incompressible periodic flow around an oscillating circular cylinder to three-dimensional perturbations can be analyzed by computing the Floquet multipliers and corresponding modes as a function of Re, β and frequency and amplitude of oscillation.

To calculate the Floquet modes, an operator representing the evolution of the system in one period is constructed:

$$\mathbf{u}'_{n+1} = \mathbf{A}(\mathbf{u}'_n), \tag{11}$$

where $\mathbf{u}'_n = \mathbf{u}'(x, y, z, t_0 + nT)$ is the perturbation vector after n periods. The eigenvalues of $\mathbf{A}$ are the Floquet multipliers of $\mathbf{L}$ and the eigenfunctions of $\mathbf{A}$ are the Floquet modes at some instant in time t_0, where t_0 depends on the initial phase of the base flow $\mathbf{U}$ used to construct $\mathbf{A}$.

The action of operator $\mathbf{A}$ on the perturbation $\mathbf{u}'$ can be computed by integrating the linearized Navier–Stokes equations, using the same schemes that were used to compute the base flow. Two changes are necessary in the integration algorithm. The first is that a linear operator $(-(\mathbf{U}.\nabla)\mathbf{u}' - (\mathbf{u}'.\nabla)\mathbf{U})$ should be used to calculate the advection terms. In this operator, the values of $\mathbf{U}$ are computed by means of a Fourier interpolation of the time slices resulting from the base flow calculation. The second change is to replace the operator ∇ by $(\partial/\partial x, \partial/\partial y, -i\beta)$, and compute the three velocity components $(\hat{u}, \hat{v}, \hat{w})$ and $\hat{p}$ on the two-dimensional domains.

Subspace iteration was used to compute the eigenvalues of $\mathbf{A}$ with largest magnitude. For all calculations, a Krylov subspace of dimension of 20 was used, initialized with $u' = 1$ and $v' = 1$ throughout the entire domain. Despite the fairly slow rate of convergence for small β, no preconditioning was applied.

2.3. Convergence analysis

The numerical method used here has been previously utilized both for direct numerical simulations [see the examples and references in Karniadakis and Sherwin (2005)] and Floquet stability calculations [see Barkley and Henderson (1996); Robichaux et al. (1999); Sheard et al. (2003); Carmo et al. (2008)]. In our investigation, we have carried out a convergence analysis following the methodology in Carmo et al. (2008). We employed 10 different meshes with different number of elements and domain sizes. We evaluated three main quantities: Strouhal number, root mean square of lift coefficient and mean drag coefficient. When these three quantities varied less than 1% from the largest and most refined mesh, we considered the result as converged. The chosen mesh had a domain size of $20d$ upstream and $40d$ downstream

with each side boundary $30d$ from the center of the cylinder. The domain is discretized in 485 elements of ninth-order polynomial interpolants. This particular mesh has been used in all simulations shown in this paper.

3. Results

3.1. Cases

The Reynolds number range of interest is the range where transition to three-dimensional flow occurs in a fixed circular cylinder case. We chose the Reynolds number of our oscillating cylinder simulations to fall in the range, $200 \leqslant \mathrm{Re} \leqslant 340$. For such Reynolds numbers, the flow around a fixed circular cylinder is already three-dimensional and this region engulfs the two-stage transition that occurs (Williamson, 1988). Experimentally, the transition between the dominance of modes A and B is observed at $\mathrm{Re} \simeq 230$–240. This choice allows the comparison between forced oscillations and fixed cylinder situations.

Meanwhile, the frequency of the forced oscillation is maintained at a fixed ratio with respect to the shedding frequency of the flow around a fixed circular cylinder. The choice of the ratio is based on the lock-in region obtained by Meneghini and Bearman (1995): we imposed a frequency ratio $f/f_S = 0.9$ which is well inside the lock-in boundary for the amplitudes of oscillation chosen in this work.

The selection of amplitude of the imposed oscillation takes into account the usual amplitude response in vortex-induced vibration; an amplitude range from $0.4d$ to $0.9d$ is a reasonable choice.

Table 1 summarizes the two-dimensional base flow cases simulated and chosen for the stability analysis. This table also presents the shedding regime as it is important of the three-dimensional mode developed. The transition between shedding modes 2S and P + S shown in Table 1 is in agreement with that presented in Leontini et al. (2006) and Table 1 extends their investigation.

3.2. Fixed cylinder results

The fixed cylinder case was used to validate the code and give a benchmark for the other cases. We followed the work by Carmo et al. (2008) employing for the Floquet analysis 32 equispaced time slices taken from a single vortex shedding period T to use in a temporal representation of the base flow. In Fig. 1, the values of the modulus of the Floquet multiplier, for these calculations, are shown. For the fixed cylinder, as can be seen analyzing Fig. 1, two different unstable modes are present in the Reynolds number range considered. These modes are called modes A and B following the nomenclature proposed by Williamson and Roshko (1988). The peaks of lowest β in each of the curves in Fig. 1 is mode A. This is the first to appear in terms of Reynolds number, and is already unstable at $\mathrm{Re} = 200$. The wavelength of maximum growth rate for this mode is about $4d$. On the other hand, mode B corresponds to the peak of higher β, having a wavelength of maximum growth rate of about $0.8d$, and it is only unstable for the case simulated with $\mathrm{Re} = 300$. These results show good agreement with those presented by Barkley and Henderson (1996).

As it was pointed out by Barkley and Henderson (1996) and Blackburn et al. (2005), another important difference (other than the wavelengths) between modes A and B is their spatio-temporal symmetries. The three-dimensional structure of the normalized Floquet mode associated with a spanwise wavenumber β can be reconstructed by considering the perturbation $\mathbf{u}'(x, y, z, t)$ in a vector form. The vorticity perturbation field can be calculated employing the modified curl vector operator applied to $\mathbf{u}'$. The T-periodic base flow follows a reflectional symmetry about the wake

Table 1
Base flow cases of a forced-oscillating circular cylinder and shedding regime obtained.

Reynolds number	Amplitude in diameters							
	0.4	0.5	0.6	0.65	0.7	0.8	0.9	1.0
200	2S	2S	2S	P + S	P + S	P + S	P + S	P + S
240	2S	2S	P + S	P + S	P + S	P + S	P + S	P + S
260	2S	2S	P + S	P + S	P + S	P + S	P + S	P + S
300	2S	2S	P + S	P + S	P + S	P + S	P + S	No pattern
340	2S	P + S	P + S	P + S	P + S	P + S	2S	No pattern

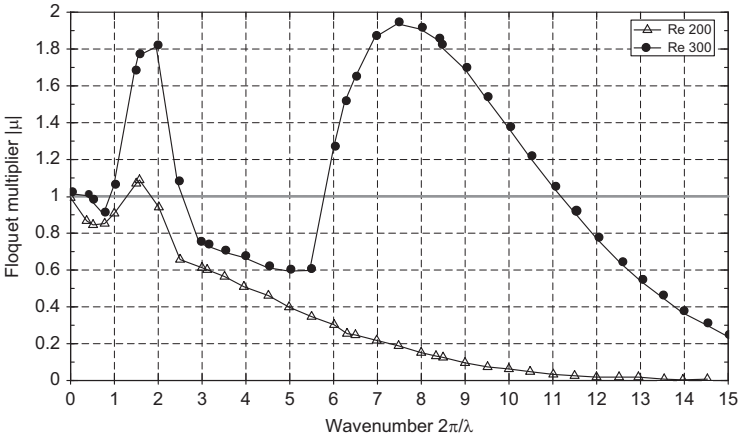

Fig. 1. Floquet multiplier μ as a function of the spanwise wavenumber β for Re = 200 and 300. Flow around a single fixed cylinder. Adapted from Carmo et al. (2008).

centerline ($y = 0$), when time is advanced by $T/2$. This symmetry is called RT symmetry (R for reflectional in space and T for translational in time) following the work by Robichaux et al. (1999). With this considerations, mode A has the following kind of symmetry

$$\text{Mode A: } \begin{cases} \tilde{u}(x,y,z,t) = \tilde{u}(x,-y,z,t+T/2), \\ \tilde{v}(x,y,z,t) = -\tilde{v}(x,-y,z,t+T/2), \\ \tilde{w}(x,y,z,t) = \tilde{w}(x,-y,z,t+T/2), \end{cases} \tag{12}$$

which is the same as the base flow, while, distinctively, mode B symmetry is

$$\text{Mode B: } \begin{cases} \tilde{u}(x,y,z,t) = -\tilde{u}(x,-y,z,t+T/2), \\ \tilde{v}(x,y,z,t) = \tilde{v}(x,-y,z,t+T/2), \\ \tilde{w}(x,y,z,t) = -\tilde{w}(x,-y,z,t+T/2). \end{cases} \tag{13}$$

Owing to the usual representation of the modes by their streamwise vorticity (ω_x) contours, the symmetries above can be rewritten using streamwise vorticity and are represented by

$$\text{Mode A: } \tilde{\omega}_x(x,y,z,t) = -\tilde{\omega}_x(x,-y,z,t+T/2) \tag{14}$$

and

$$\text{Mode B: } \tilde{\omega}_x(x,y,z,t) = \tilde{\omega}_x(x,-y,z,t+T/2). \tag{15}$$

The results shown in Fig. 1 and all comments regarding symmetry properties of modes A and B of the fixed cylinder will serve us for further comparison with the oscillating circular cylinder flow investigated in the present work. Just to complete the kinds of symmetry, the subharmonic mode (when Floquet multiplier is real and negative) has its symmetry represented by

$$\text{Subharmonic mode: } \tilde{\omega}_x(x,y,z,t) = \tilde{\omega}_x(x,y,z,t+2T). \tag{16}$$

3.3. Oscillating circular cylinder results

After reviewing the single fixed circular cylinder case, we now proceed to analyze the stability of the periodic flow around an oscillating cylinder. Under low amplitudes of oscillations, the wake of the circular cylinder sheds a pair of vortices every cycle of oscillation (see Table 1). It is reasonable to expect a similar behavior of this wake and the wake of a fixed circular cylinder.

As seen in Fig. 2, the oscillation of the body delays the secondary transition with respect to Reynolds number. The wake of the oscillating circular cylinder at amplitude $0.4d$ is stable with respect to infinitesimal three-dimensional perturbations for Reynolds number up to around 260. The oscillatory motion has a stabilizing action on the wake at

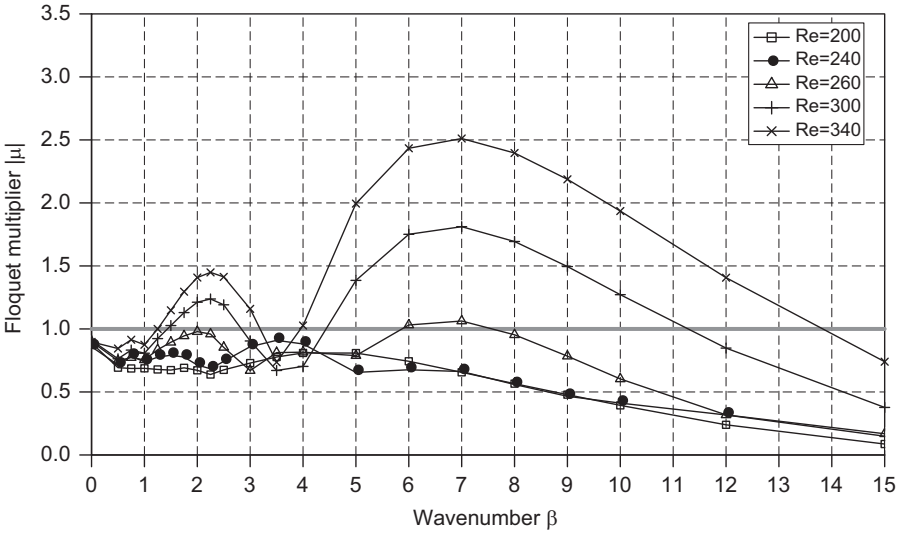

Fig. 2. Floquet multipliers $|\mu|$ as function of wavenumber β for an oscillating circular cylinder with amplitude $0.4d$.

such low amplitudes. This means that all three-dimensionalities decay as it was also observed by Gioria and Meneghini (2007).

For higher Reynolds numbers (300 and 340 shown in Fig. 2), the wake dynamics is similar to the fixed cylinder case. Two peaks of the most unstable wavelength are observed. These two peaks, corresponding to modes A and B, are clearly evident. However, there are some significant changes. The two peaks on the graph are at $\beta \approx 2.25$ and 7.0, which correspond to $\lambda \approx 2.8d$ and $0.9d$, respectively. Only the latter resembles mode B with respect to the wavelength. The former has a wavelength quite different from the one found in mode A although for a stationary cylinder the preferred wavelength decreases with increasing Reynolds number. Despite this difference in the wavelength, the symmetry of the wake can be represented in the same way as mode A (see Eq. (14)). This is shown in Fig. 3(a), where the instantaneous streamwise vorticity field is overlaid with spanwise vorticity contours of the base flow. This figure also indicates that the unstable mode is more intense in the braid shear layer, which is another remarkable difference from mode A for a stationary cylinder.

Concerning the shorter unstable wavelength, its wake mode symmetry is similar to mode B symmetry observed for a fixed cylinder wake. Also, it is stronger in the braid shear layers.

As we move to higher amplitudes, a change in the wavelengths of the instability occurs and the critical Reynolds number is modified. Analyzing the results shown in Fig. 4(a), it is possible to conclude that the cases with amplitude of oscillation $A/d = 0.5$, and $\mathrm{Re} = 200$ and 240, are stable with respect to three-dimensional perturbations. As the Reynolds number is increased to 260, the wake becomes marginally stable. The case $\mathrm{Re} = 300$ becomes unstable and two peaks of the most unstable wavelength are observed, similarly to what has been noticed previously for the case $A/d = 0.4$ and same Reynolds number.

A remarkable change in the stability properties happens in the case $A/d = 0.5$ and $\mathrm{Re} = 340$. This change is related to the switch of mode patterns of vortex shedding: the case $\mathrm{Re} = 340$ and $A/d = 0.5$ has a P + S pattern, and all other cases discussed so far had a 2S mode (see Table 1).

Fig. 4(a) explicitly shows the effect of the amplitude of oscillation on the instability wavenumber for the case with $\mathrm{Re} = 340$ (line with $\times$ markers). In this figure we can see another noticeable difference between this case and all previous cases: the $\mathrm{Re} = 340$ case has a single unstable peak located at $\beta \approx 4$, which corresponds to a wavelength $\lambda \approx 1.57d$. This means that the transition only occurs through 1 kind of mode, different than what is observed for a fixed circular cylinder for the same Reynolds number as noted in Section 3.2, which shows two unstable modes.

It is important to notice that the Floquet multipliers in this case are all real and negative leading to a subharmonic mode. According to Blackburn et al. (2005), this subharmonic mode is not possible to occur if the wake possesses the spatio-temporal symmetry of the typical von Kármán wake (half period time shift and spatial reflection about wake centerline); the P + S shedding pattern does not possess this spatio-temporal symmetry thus it may have unstable subharmonic modes. This change is repeated for other Reynolds numbers as the amplitude is increased: in Fig. 4(b) shows that the Reynolds number 200 case at last suffers this change in wavelength with oscillation amplitude around

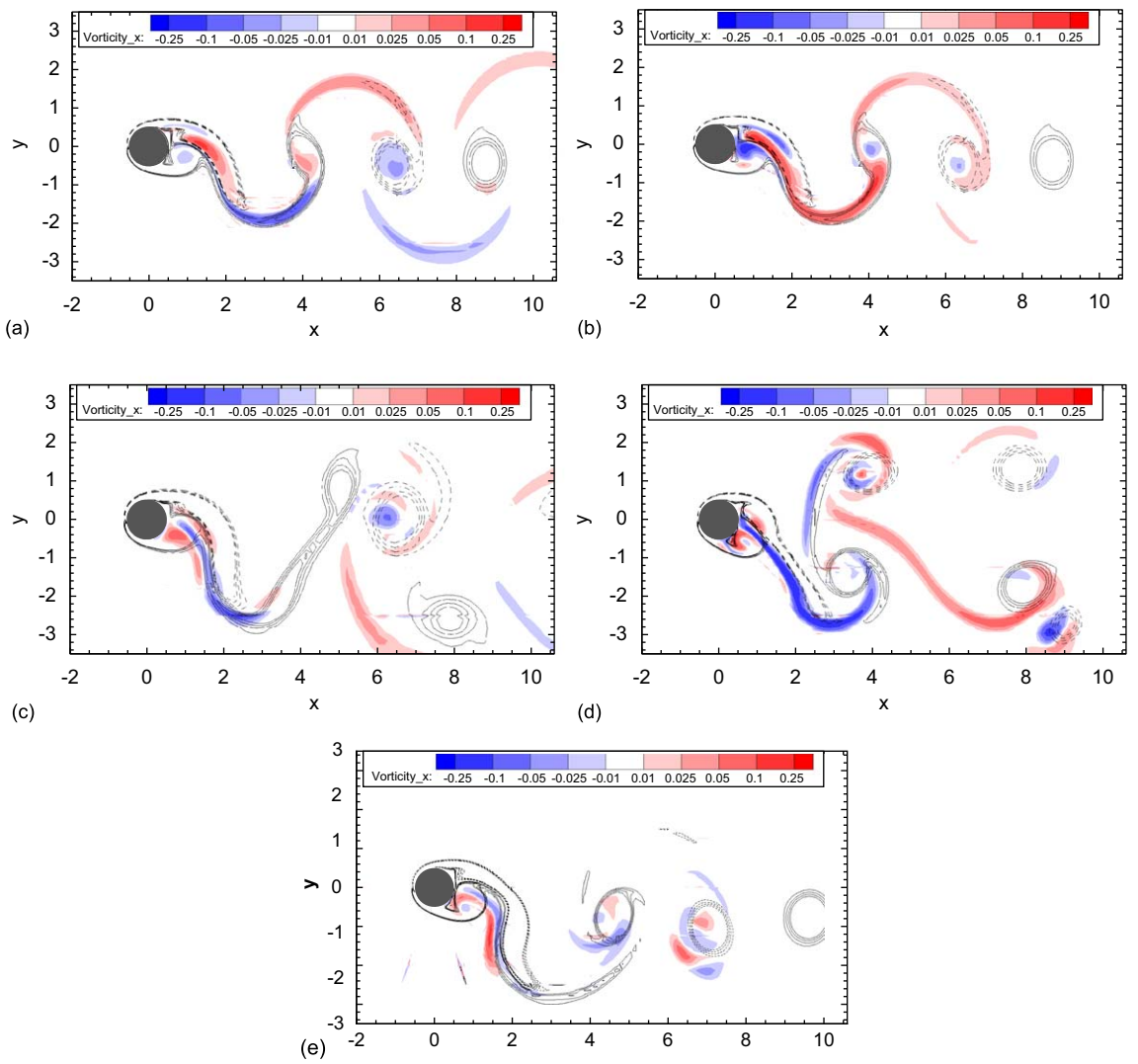

Fig. 3. Instantaneous streamwise vorticity field ($\omega_x d/U_\infty$, from negative values in blue, through null in white, to positive ones in red) superposed to spanwise vorticity of the base flow ($\omega_z d/U_\infty$, from negative values in dashed lines to positive ones in full lines). The spanwise location is where the vorticity field is more intense. (a) $\mathrm{Re} = 300$, $A/d = 0.4$, $\beta = 2.25$. (b) $\mathrm{Re} = 300$, $A/d = 0.4$, $\beta = 7.00$. (c) $\mathrm{Re} = 200$, $A/d = 0.7$, $\beta = 4.00$. (d) $\mathrm{Re} = 300$, $A/d = 0.7$, $\beta = 9.00$. (e) $\mathrm{Re} = 340$, $A/d = 0.9$, $\beta = 8.00$ (For interpretation of the references to color in this figure legend, the reader is referred to the web version of this article.).

$0.65d$. The change in the three-dimensional mode is accompanied by the change in the two-dimensional vortex shedding pattern from 2S to P + S. The subharmonic mode that arises in this instability is shown in Fig. 3(c) and it is also stronger in the braid shear layers linking. The same was observed in previous works in which such subharmonic mode was observed (Sheard et al., 2003; Carmo et al., 2008; Leontini et al., 2007).

As the amplitude is increased from $0.5d$ to $0.7d$ (Fig. 4(a) and (b)), there is another difference observed in the results. At $\mathrm{Re} = 300$ and 340, for $A/d = 0.7$, two peaks are observed. These peaks have multipliers which are real positive and real negative, respectively, in ascending order of wavenumber β. The case of highest β and negative multiplier, for $A/d = 0.7$ and $\mathrm{Re} = 300$, is shown in Fig. 3(d).

At last, for amplitude $0.9d$ in the highest Reynolds number case, the vortex shedding pattern suffers another change. The pattern backtracks to a 2S shedding pattern. The Floquet multiplier versus wavenumber graph does not change its looks: it still has two peaks around wavenumber approximately 1.25 and 9. Interestingly, but still in agreement with

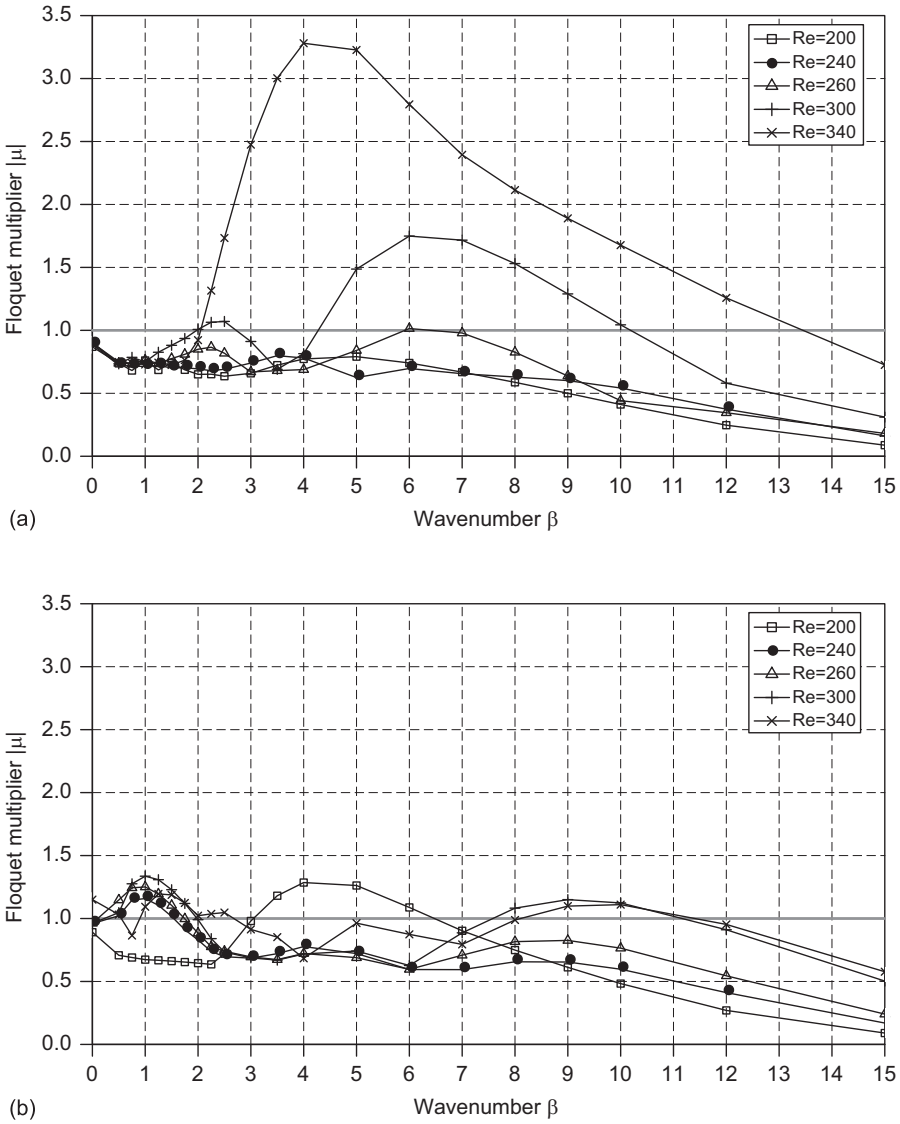

Fig. 4. Floquet multipliers $|\mu|$ as function of wavenumber β for an oscillating circular cylinder. (a) $A/d = 0.5$. (b) $A/d = 0.7$.

Blackburn et al. (2005), the highest wavenumber peak is not a subharmonic mode anymore, it has complex Floquet multipliers and is a quasi-periodic mode. Fig. 3(e) shows this Floquet quasi-periodic mode.

4. Conclusion

The results presented here show that the wake transition in the flow around an oscillating cylinder is remarkably different from that in the flow around a fixed cylinder. The stability of the flow with respect to three-dimensional perturbations and the topology of the unstable modes observed are highly dependent on the amplitude of vibration and vortex shedding mode.

For small amplitudes, $A/D = 0.4$ and 0.5, the vibration of the body can make the flow more stable. For example, for $200 \leqslant \mathrm{Re} \leqslant 260$ the flow was stable for these amplitudes. For this Reynolds number range, the flow of an non-oscillating cylinder is already unstable to three-dimensional perturbations.

If the amplitude was increased, the vortex shedding regime changed from 2S to P + S, and the stability of the flows were dramatically altered. In general, for this shedding regime two different scenarios were observed. For smaller amplitudes, the graphs of $|\mu(\beta)|$ exhibited just one peak for intermediate wavenumbers. This was a period-doubling mode (μ real and negative) and it was stronger in the braid shear layers that linked vortices of different vorticity signs and located at opposite sides of the wake (see Fig. 3(c)).

The second scenario for P + S shedding mode happened for higher amplitudes. In this case, two different peaks were observed. One for small β, which has a mode A character (real positive Floquet multiplier). The other has a wavenumber closer to mode B, however, differently from mode B, it is a period-doubling mode. This difference is caused by the asymmetry in the wake (P + S vortex shedding pattern), which prevents a strong interaction between the shear layers of two consecutive shedding cycles. We wonder if the lack of such feedback could lead to an alternation of sign from cycle to cycle.

A further increase in the amplitude makes the vortex-shedding regime to be 2S again. However, the wake transition was completely different from what was observed for small amplitudes.

Acknowledgments

We would like to acknowledge the useful comments of Prof. J.A.P. Aranha and Dr. R. Willden concerning the numerical method and the simulation results, and Prof. S. Sherwin, for providing the Nektar code in an early stage of this research project. R.S.G., P.J.S.J. and B.S.C. would like to acknowledge Fapesp and Capes for the scholarships that were provided during the development of this work. J.R.M. would like to acknowledge the financial support by FINEP, CNPq, and Petrobras. All the computing resources were provided by NDF-University of São Paulo.

References

Barkley, D., Henderson, R.D., 1996. Three-dimensional Floquet stability analysis of the wake of a circular cylinder. Journal of Fluid Mechanics 322, 215–241.

Bearman, P.W., Currie, I.G., 1979. Pressure fluctuation measurements on an oscillating circular cylinder. Journal of Fluid Mechanics 91 (4), 661–677.

Blackburn, H.M., Henderson, R.D., 1999. A study of two-dimensional flow past an oscillating cylinder. Journal of Fluid Mechanics 385, 255–286.

Blackburn, H.M., Marquez, F., Lopez, J.M., 2005. Symmetry breaking of two-dimensional time-periodic wakes. Journal of Fluid Mechanics 522, 395–411.

Carmo, B.S., Sherwin, S.J., Bearman, P.W., Willden, R.H.J., 2008. Wake transition in the flow around two circular cylinders in staggered arrangements. Journal of Fluid Mechanics 597, 1–29.

Gioria, R.S., Carmo, B.S., Meneghini, J.R., 2007a. Floquet stability analysis of the flow around an oscillating cylinder. In: BBVIV-5, Brazil.

Gioria, R.S., Carmo, B.S., Meneghini, J.R., 2007b. Three-dimensional wake structures of flow around an oscillating circular cylinder. In: Proceedings of OMAE 2007: 26th International Conference on Offshore Mechanics and Arctic Engineering. ASME, San Diego, USA.

Gioria, R.S., Meneghini, J.R., 2007. Three-dimensionalities of the flow around an oscillating circular cylinder. In: IUTAM Symposium on Unsteady Separated Flows and their Control, Corfu, Greece (poster presentation).

Griffin, O.M., Ramberg, S.E., 1974. The vortex-street wakes of vibrating cylinders. Journal of Fluid Mechanics 66, 553–576.

Griffin, O.M., Skop, R.A., Koopman, G.H., 1973. The vortex-excited resonant vibrations of circular cylinders. Journal of Sound and Vibration 31, 235–249.

Henderson, R.D., 1997. Nonlinear dynamics and pattern formation in turbulent wake transition. Journal of Fluid Mechanics 352, 65–112.

Henderson, R.D., Barkley, D., 1996. Secondary instability of the wake of a circular cylinder. Physics of Fluids 8 (6), 65–112.

Iooss, G., Joseph, D.D., 1990. Elementary Stability and Bifurcation Theory. Undergraduate Texts in Mathematics, second ed. Springer, Berlin.

Karniadakis, G.E., Israeli, M., Orszag, S.A., 1991. High-order splitting methods for the incompressible Navier–Stokes equations. Journal of Computational Physics 97, 414–443.

Karniadakis, G.E., Sherwin, S.J., 1999. Spectral/*hp* Element Methods for CFD. Oxford University Press, New York.

Karniadakis, G.E., Sherwin, S.J., 2005. Spectral/*hp* Element Methods for CFD, second ed. Oxford University Press, New York.

Leontini, J.S., Stewart, B.E., Thompson, M.C., Hourigan, K., 2006. Wake state and energy transitions of an oscillating cylinder at low Reynolds number. Physics of Fluids 18 (6), 067101.

Leontini, J.S., Thompson, M.C., Hourigan, K., 2007. Three-dimensional transition in the wake of a transversely oscillating cylinder. Journal of Fluid Mechanics 577, 79–104.

Leweke, T., Williamson, C.H.K., 1998. Three-dimensional instabilities in the wake transition. European Journal of Mechanics B: Fluids 4, 571–586.

Li, L., Sherwin, S.J., Bearman, P.W., 2002. A moving frame of reference algorithm for fluid/structure interaction of rotating and translating bodies. International Journal of Numerical Methods in Fluids 38, 187–206.

Meneghini, J.R., Bearman, P.W., 1995. Numerical simulation of high amplitude oscillatory flow about a circular cylinder. Journal of Fluids and Structures 9, 435–455.

Robichaux, J., Balachandar, S., Vanka, S.P., 1999. Three-dimensional Floquet instability of the wake of a square cylinder. Physics of Fluids 11 (3), 560–578.

Sheard, G.J., Thompson, M.C., Hourigan, K., 2003. From spheres to circular cylinders: the stability and flow structures of bluff ring wakes. Journal of Fluid Mechanics 492, 147–180.

Sheard, G.J., Thompson, M.C., Hourigan, K., 2005. Subharmonic mechanism of the mode C instability. Physics of Fluids 17 (11) Art. No. 111702.

Thompson, M.C., Hourigan, K., Sheridan, J., 1996. Three-dimensional instabilities in the wake of a circular cylinder. Experimental Thermal and Fluid Science 12 (2), 190–196.

Williamson, C., Roshko, A., 1988. Vortex formation in the wake of an oscillating cylinder. Journal of Fluids and Structures 2, 355–381.

Williamson, C.H.K., 1988. The existence of two stages in the transition to three-dimensionality of a cylinder wake. Physics of Fluids 31 (11), 3165–3168.

Williamson, C.H.K., 1996. Three-dimensional wake transition. Journal of Fluid Mechanics 328, 345–407.

Wu, J., Welch, L.W., Welsh, M.C., Sheridan, J., Walker, G.J., 1994. Spanwise wake structures of a circular cylinder and two circular cylinders in tandem. Experimental Thermal and Fluid Science 9 (3), 299–308.

Zhang, H.Q., Fey, U., Noack, B.R., König, M., Eckelman, H., 1995. On the transition of the cylinder wake. Physics of Fluids 7 (4), 779–794.